Journal of Materials Chemistry A

COMMUNICATION

View Article Online
View Journal | View Issue

Cite this: J. Mater. Chem. A, 2018, 6, 3361

Received 21st December 2017
Accepted 24th January 2018

DOI: 10.1039/c7ta11139h

rsc.li/materials-a

A solar actuator based on hydrogen-bonded azopolymers for electricity generation†

Yubing Xiong, ‡[ac] Lidong Zhang,‡[bd] Philipp Weis,[a] Panče Naumov *[b] and Si Wu *[a]

An actuator driven by solar light is developed by incorporating an azo compound (F-Azo) into agarose (AG). The resulting F-Azo-doped AG (F-Azo@AG) films bend under sunlight irradiation. It is demonstrated that the sunlight-induced bending of the F-Azo@AG film transduces the sunlight into electricity when attached to a piezoelectric transducer.

Phototropic plants that respond to sunlight with mechanical motion—the sunflower (*Helianthus annuus*) being the most common example—inspire the design of photoactuators[1–5] which convert sunlight into mechanical motion. Artificial photoactuators are based on a variety of photoactive materials including gels,[6–8] crystals,[9,10] and liquid crystal elastomers (LCEs).[3,5,11–17] Exposure of photoactuators to light can induce bending,[3,9] contraction,[5] rotation,[15,18] oscillation,[19] twisting,[17,20] and other motions[21,22] that are essential to applications in microfluidic devices,[12] motors,[18] and electrical generators.[23–25] Due to advantages such as ease of preparation and controllable motility, photoactive LCEs are particularly promising for photoactuating materials. Most of the currently known light-driven LCEs have been constructed by introducing azobenzenes into polymer networks.[1–3,5,11–19,21–25] The *trans*-to-*cis* isomerization under UV light and *cis*-to-*trans* isomerization with visible light makes the azobenzene group a robust, durable, and fatigueless photoswitchable unit that is now ubiquitous in photoactive materials.[26–28] *trans*-Azobenzene is a liquid crystal mesogen, which stabilizes liquid crystal phases, while the *cis*-azobenzene is not a liquid crystal mesogen and usually destabilizes the liquid crystal phases.[29] Thus, *trans*-to-*cis* photoisomerization of azobenzene groups in LCEs can induce liquid-crystal-to-isotropic phase transition, which results in reshaping of the LCEs that manifests as mechanical motion.[1] Additionally, the photoisomerization of azobenzene has been widely utilized to control the state, morphology, and size of polymer matrices.[30–34] Since the *trans*-to-*cis* isomerization is induced by UV light, the UV light is normally the first choice as a stimulus to actuate azobenzene-based LCEs.[1] Lasers at visible wavelengths, which can induce *trans–cis–trans* cycling of azobenzene groups in LCEs have also been used.[19] Since the sun is a cost-free source of energy, using sunlight is a comparatively much more energy-efficient approach to photoactuation. Because visible light comprises the majority of the solar spectrum, azotolane derivatives responsive to wavelengths that are red-shifted relative to the absorption of conventional azobenzenes were prepared and introduced into LCEs.[35–37] It was shown that—after being concentrated by lenses and filtered to a suitable wavelength range—sunlight can indeed induce bending of such azotolane-containing LCEs.[35,36] Recently, tetra-*ortho*-substituted azobenzenes that can be switched solely by visible light were developed.[38–46] Kumar *et al.*[47] fabricated *ortho*-fluoroazobenzene-containing LCEs and showed that non-concentrated sunlight induces chaotic oscillations with relatively small amplitudes. While sunlight-induced motion has already been demonstrated, the development of solar actuators with controlled and enhanced motions for efficient solar energy conversion remains a challenge.

In this work, by using a fundamentally different approach from that used in photoactuating LCEs, we succeeded in developing a new actuator that is driven by sunlight. Unlike ordinary LCEs, the new photoactive material does not require alignment of chromophores and crosslinking, making the solar actuator better suited for implementation in devices. Importantly, we also demonstrated that sunlight-induced bending of the new actuator is efficient enough to generate electricity. The

[a]Max Planck Institute for Polymer Research, Ackermannweg 10, Mainz 55128, Germany. E-mail: wusi@mpip-mainz.mpg.de

[b]New York University Abu Dhabi, PO Box 129188, Abu Dhabi, United Arab Emirates. E-mail: pance.naumov@nyu.edu

[c]Department of Chemistry, Zhejiang Sci-Tech University, Hangzhou 310018, Zhejiang Province, China

[d]Department of Chemistry and Molecular Engineering, East China Normal University, Shanghai 200241, China

† Electronic supplementary information (ESI) available. See DOI: 10.1039/c7ta11139h

‡ These authors contributed equally to this work.

actuator (F-Azo@AG) was fabricated by introducing 2,2′,6,6′-tetrafluoro-4,4′-diacetamidoazobenzene (F-Azo) into agarose (AG) as the matrix (Fig. 1). The absorption spectrum of F-Azo overlaps with the solar spectrum better than the azobenzene (Fig. S1†) and its photoisomerization can be induced with sunlight. AG was used as the matrix based on previous results showing that when combined with photoswitchable molecules such as 1,4-bis(*para*-hydroxystyryl)benzene or azobenzene derivatives, AG is a mechanically compliant matrix that can be efficiently actuated.[20,22] The hydrogen bonding network of AG provides both moderate mechanical strength and softness required for photoactuation. Furthermore, the F-Azo@AG film was coupled to a polyvinylidene difluoride (PVDF) film that acts as a piezoelectric transducer (Fig. 1). PVDF is a dielectric material capable of generating electric current when subjected to external mechanical force.[48–50] Upon irradiation with sunlight, the bending of the F-Azo@AG film drives bending of the PVDF piezoelectric transducer, resulting in generation of electricity.

F-Azo was synthesized by coupling 2,6-difluoro-4-bromoaniline followed by substitution with acetamide (for details, see the ESI, Fig. S2†).[39] The *trans* isomer of F-Azo has a π–π* absorption band in the UV region and an n–π* band in the visible region (Fig. 2b). Thus, F-Azo can absorb sunlight from the UV region to around 600 nm in the visible range. When compared to azobenzene, F-Azo has a more intense and red-shifted absorption band in the visible range (Fig. S1†), making F-Azo a better suited chromophore for sunlight harvesting.

The photoisomerization was also quantitatively studied using ^{1}H NMR spectroscopy (Fig. 2c). The signals of F-Azo at 10.65, 7.50 and 2.12 ppm are ascribed to H 1, 2, and 3, respectively (Fig. 2a). After F-Azo was irradiated with green light (530 nm, 4.94 mW cm^{-2}), three new signals of the *cis* isomer at 10.48, 7.33, 2.05 ppm appeared. Integration showed that ~75% of the molecules exist as the *cis* isomer in the photostationary state. Subsequent irradiation with blue light (470 nm, 2.23 mW cm^{-2}) reduced the *cis* content to ~44% at the photostationary state. Because both *trans* and *cis* isomers absorb blue light, the concomitant *trans*-to-*cis* and *cis*-to-*trans* isomerization induced by blue light resulted in a mixture of the isomers. Complete *cis*-to-*trans* isomerization was accomplished by heating the sample at 90 °C for 30 min. Interestingly, approximately 62% *cis* isomer was obtained when *trans*-F-Azo was irradiated with a solar simulator to a photostationary state, which indicated that sunlight can induce *trans*-to-*cis* isomerization of F-Azo.

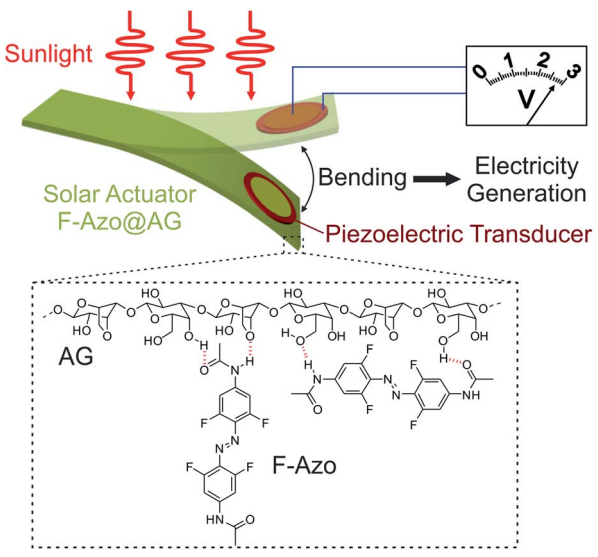

Fig. 1 Schematic illustration of the conversion of sunlight into electric power by combining a solar actuator with a piezoelectric transducer. The solar actuator is a supramolecular film of the sunlight-responsive azo compound (F-Azo) hydrogen-bonded with the agarose (AG) matrix. The piezoelectric transducer is polyvinylidene difluoride (PVDF). The bending of the actuator under solar irradiation leads to bending of the piezoelectric transducer and subsequent generation of electricity.

Encouraged by this result, we introduced F-Azo into the AG matrix to prepare a solar actuator F-Azo@AG which contains ~1.1 wt% F-Azo. When more F-Azo is introduced, it will crystallize in the AG matrix. As a result, the bending of the film will be weakened. The F-Azo@AG films were prepared by mixing F-Azo and AG in *N*,*N*-dimethyl formamide, casting the mixture on glass slides, and drying at room temperature over two days. Free-standing F-Azo@AG films were obtained by peeling the films off the glass substrates and stored in a desiccator. Firstly, the film was measured using UV spectroscopy. As illustrated in Fig. S3,† the *trans* absorption decreased and the *cis* absorption increased simultaneously when the film was illuminated by green light. The F-Azo@AG film was also examined using a solar simulator. As shown in Fig. S4,† the *trans* absorption of the film attenuated when it was exposed to the solar simulator. The results demonstrated that the *trans*-to-*cis* isomerization of F-Azo in the film could be achieved under the irradiation of green light and solar simulator. The motion of a free-standing F-Azo@AG film (20 mm × 20 mm × 40 μm) was studied by exposing the film to light from a solar simulator (Fig. 3a and Movie 1†). The film responded by bending along its centreline with small oscillations. The film bends towards the sunlight and is thus phototropic. After irradiation for a few seconds, the film reached maximal deflection with only small amplitude oscillations. Subsequently, the film was flipped and its reverse side was exposed to light from the solar simulator (Fig. 3a(IV)). The film unbent until it became nearly flat (Fig. 3a(VI)), and then bent towards the sunlight (Fig. 3a(VII)). The result confirms that sunlight can indeed induce bending of the F-Azo@AG film.

The mechanism of operation of AG-based actuators is qualitatively different from that of LCEs. It is well known that the orientation of liquid crystal mesogens controls the bending of LCEs.[1,3] In contrast, the F-Azo@AG film was dark under polarized light, indicating that F-Azo is distributed homogeneously in the AG matrix and does not have any preferred orientation (Fig. S5†).

The bending of AG-based actuators is usually affected by their shapes, imperfections in the fabrication process, and creases on the actuators. Previous work has shown that the shape of AG-based actuators is the primary factor that determines their bending performance.[20,22] To investigate these

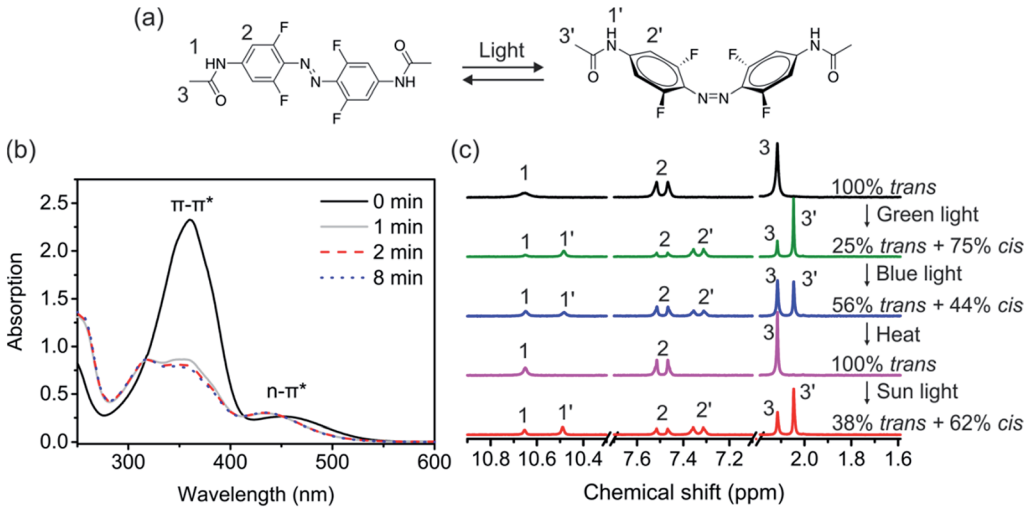

Fig. 2 (a) Photoisomerization of F-Azo. (b) UV-vis absorption spectra of F-Azo in DMSO before irradiation and after irradiation with green light (530 nm, 4.94 mW cm^{-2}) for 1 min, 2 min, and 8 min. (c) ^{1}H NMR spectra (DMSO-d_6) of F-Azo under different treatments (from top to down): 100% *trans* F-Azo; after green light (530 nm, 4.94 mW cm^{-2}) irradiation to the photostationary state; after blue light (470 nm, 2.23 mW cm^{-2}) irradiation to the photostationary state; after heating at 90 °C for 30 min; after the irradiation with sunlight from a solar simulator (76.6 mW cm^{-2}) to the photostationary state. The hydrogens on *trans* and *cis* F-Azo are labelled with 1, 2, 3, 1′, 2′, and 3′.

effects, the response to sunlight of F-Azo@AG films with different shapes were studied. F-Azo@AG films were cut into strips with a fixed length and different widths (length, 7 mm; width, 1, 3, or 5 mm) and clamped using a support (Fig. 3b). Their bending performance under simulated sunlight (76.6 mW cm^{-2}) was quantified (Fig. 3c and Movies 2–4†). The bending rate of the 1 mm-wide strip was the fastest and its tip deflection was also the largest. As the width of the strip increased to 3 and 5 mm, the bending rate and tip deflection gradually reduced. This result shows that the bending of F-Azo@AG strips is dependent on their shape. When the width increases, the aspect ratio decreases as the short side of the strip becomes close in length to the long side. The stress for bending along the longitudinal direction becomes comparable to that along the transverse direction. The strip has a tendency to bend and oscillate in both the longitudinal and the transverse directions. Although fixing of one end of the 5 mm-wide strip using a clamp hindered its motion along the longitudinal

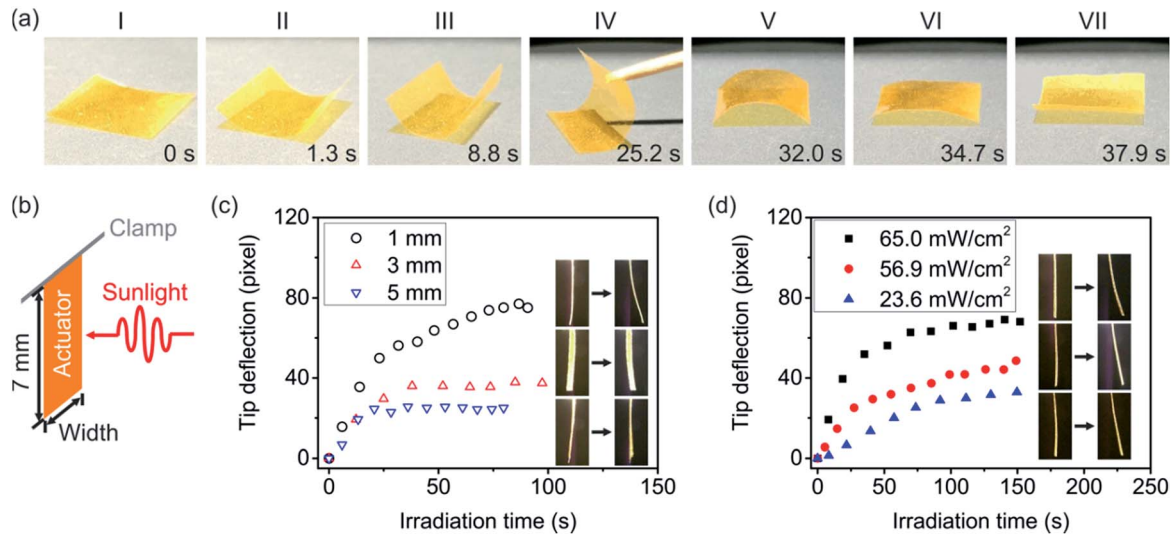

Fig. 3 (a) Snapshots of sunlight-driven bending of a F-Azo@AG film (20 mm × 20 mm × 40 μm). From (I) to (III), the film was irradiated using a solar simulator from the top. At stage (IV), the film was flipped over. From (V) to (VII), the reverse side of the film was illuminated by the solar simulator (76.6 mW cm^{-2}). (b) Setup used for quantification of the bending of F-Azo@AG strips under light from a solar simulator. (c) Effects of the width of the F-Azo@AG strips on their bending performance under light from a solar simulator (76.6 mW cm^{-2}). The length of the strips is 7 mm and their widths are 1, 3, and 5 mm, respectively. (d) Bending performances of 7 mm × 1 mm F-Azo@AG strips under different sunlight intensities. The thicknesses of the strips are ~40 μm. Insets in panels (c) and (d) show the snapshots of the strips before and after irradiation. The snapshots were taken from Movies 1–7 in the ESI.†

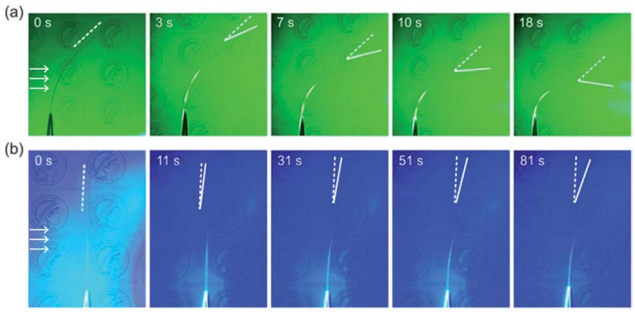

Fig. 4 Snapshots of bending of F-Azo@AG films (40 mm × 5 mm × 30 μm) induced by (a) green light (530 nm) and (b) blue light (470 nm). The snapshots were taken from Movies 9 and 10 in the ESI.† The arrows show the irradiation direction.

direction, the motion of the 5 mm-wide strip under irradiation was irregular (Movie 4†). This result shows that the bending performance of F-Azo@AG actuators can be controlled by changing their shape.

The bending performance of F-Azo@AG actuators can also be controlled by adjusting the light intensity. The bending performances of F-Azo@AG strip (7 mm × 1 mm × 40 μm) was studied by irradiation with simulated sunlight with different intensities (Fig. 3d and Movies 5–7†). When the light intensity was increased, the bending rate and the tip deflection also increased. This result shows that higher light intensity stimulates more pronounced optomechanical response.

To understand the mechanism of sunlight-induced motility, an AG film without F-Azo was irradiated with sunlight and its response was observed as a control (Fig. S6 and Movie 8†). Irradiation of the AG film induced very small oscillations (tip deflection < 3 pixels). However, no bending was observed. This result confirms that the bending of the hybrid films is due to the presence of F-Azo. The minor oscillations reflect temporal instability which could be due to strains caused by photothermal effects. A comparison with earlier studies sheds some light on these effects. Although the motility of many azobenzene-based LCEs is due to a transition of the liquid crystal phase to the isotropic phase based on *trans*-to-*cis* photoisomerization,[18] photothermal effects cannot be excluded. For example, Zhao's group reported photoinduced contraction of LCEs originating from both photoisomerization of azobenzene and a photothermal effect.[15] Priimägi and collaborators demonstrated that LCEs doped with an azo dye showed photoinduced bending due to a photothermal effect.[51] To assess the photothermal effects, the F-Azo@AG film was studied using an infrared thermometer. Irradiating a F-Azo@AG film with simulated sunlight at 76.6 mW cm^{-2} increased the sample temperature by 3 °C (Fig. S7†). Our previous work has shown that direct heating of AG-based actuators of up to 6 °C does not result in bending.[20,22] Importantly, irradiating the AG film did not result in bending (Fig. S6 and Movie 8†). Taken together, these results discredit the photothermal effects in F-Azo@AG as a major contributor to the motion of the film.

We verified the effects of photoisomerization by irradiating F-Azo@AG film with light of different wavelengths (Fig. 4, Movies 9 and 10†). Irradiating the F-Azo@AG film with green light ($\lambda = 530$ nm, 16.5 mW cm^{-2}) for 18 s resulted in a bending angle of 52° (Fig. 4a and Movie 9†). The bent film was unable to straighten to the initial state spontaneously, suggesting that bending is due to the existence of the *cis* form. In contrast, exposure of the F-Azo@AG film to blue light (14.8 mW cm^{-2}) for 81 s resulted in a bending angle of 15° (Fig. 4b and Movie 10†). The bending induced with blue light was slower and had smaller amplitude than when induced with green light. Although F-Azo can absorb more blue light than green light (Fig. 2b), the *trans*-to-*cis* isomerization is more efficiently induced with green light (Fig. 2c). The wavelength-dependent bending reveals that more efficient *trans–cis* isomerization leads to more efficient bending. These results also suggest that the photoisomerization plays an important role in the bending of F-Azo@AG, although the photothermal effect may synergistically induce some motion. The actual mechanism by which the hydrogen bonding network mediates the transfer of a momentum from the photoswitchable chromophores to the matrix within the reported AG-based actuators remains unclear and is a subject of ongoing research.

The most immediate application of sunlight-induced motions is conversion of solar light into another, useful form of energy. For this purpose, an F-Azo@AG film was mechanically coupled with a PVDF piezoelectric transducer (Fig. 5a). A weight

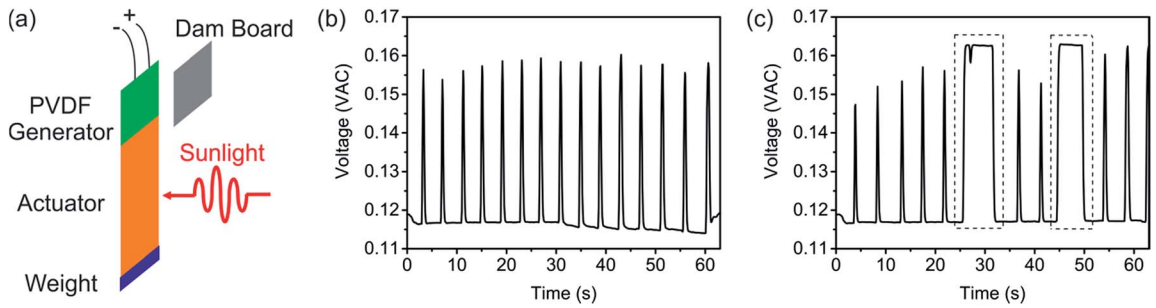

Fig. 5 Sunlight-induced actuation for electricity generation. (a) Schematic illustration of the device used for solar energy conversion. When the solar simulator is switched on, the instant bending moment of the actuator is transferred to the PVDF piezoelectric transducer, where the mechanical energy is converted into electric energy. (b) Open-circuit voltage signals are generated by the device at the sunlight exposure interval of every 3 s. (c) Open-circuit voltage signals showing continuous generation of electricity when the light from the solar simulator was kept on continuously for 6 s (highlighted with dashed lines).

was attached to the bottom of the F-Azo@AG film, which stabilized the vibration of the generator. Tensile testing (Fig. S8†) confirmed that F-Azo@AG film was hard enough to transfer the photostress to the PVDF piezoelectric transducer. F-Azo@AG film was also analyzed using a differential scanning calorimeter (DSC). As illustrated in Fig. S9,† no endothermic melting peaks could be observed in the curves before and after light irradiation. The results demonstrated that there were no F-Azo crystals in the AG matrix, *i.e.* F-Azo was homogeneously dispersed in the AG matrix. When the film was exposed briefly to solar light, it instantly generated a bending movement that was transferred to the PVDF generator, resulting in an open-circuit alternating voltage signal. When the solar simulator was switched on in an interval of every 3 s, alternating voltage signals were generated with the same interval (Fig. 5b). To test if sunlight could drive the device for continuous generation of alternating voltage signal, the solar simulator was switched on for 6 s. A stable alternating voltage signal of 0.164 V was generated continuously for 6 s, indicating that the electricity generation could be accurately controlled by controlling the sunlight exposure time (Fig. 5c, dashed lines). A control experiment performed in the dark confirmed that the electricity generation is due to photoactuation (Fig. S10†).

Conclusions

In summary, a novel solar actuator F-Azo@AG was fabricated by introducing sunlight-responsive F-Azo into the AG matrix. Sunlight can efficiently induce bending of the actuator. To demonstrate the use of F-Azo@AG for solar energy conversion, F-Azo@AG film and a piezoelectric transducer were coupled into an electrical generator which converts the sunlight-driven motion of F-Azo@AG into electricity. The design principle for F-Azo@AG is fundamentally different from that of LCEs; notably, F-Azo@AG does not require prealignment of the chromophores and crosslinking, which facilitates the fabrication of devices. Compared with a humidity-driven electricity generator based on AG,[20,22] the solar actuator operates in a dry environment, which can be easily accomplished with simple electronics without hazards with short circuits. The main asset of the F-Azo@AG actuator, however, is its ability to harness solar energy. Within a broader context, this work provides a new strategy for designing solar actuators and demonstrates the application of actuators to solar energy conversion.

Conflicts of interest

There are no conflicts to declare.

Acknowledgements

This work was supported by the Deutsche Forschungsgemeinschaft (DFG, WU 787/2-1), National Natural Science Foundation of China (Grant No. 21774101, 21474080, 51603068), and Natural Science Foundation of Shanghai (Grant No. 17ZR1440600). This research was partially financially supported by the National Research Foundation of the UAE (UIRCA 2014-683) and with a Research Enhancement Fund from NYU Abu Dhabi. Dr Y. Xiong acknowledges the financial support by the CSC program. Open Access funding was provided by the Max Planck Society.

References

1 T. Ikeda, J. Mamiya and Y. Yu, *Angew. Chem., Int. Ed.*, 2007, **46**, 506–528.
2 D. Habault, H. Zhang and Y. Zhao, *Chem. Soc. Rev.*, 2013, **42**, 7244–7256.
3 Y. L. Yu, M. Nakano and T. Ikeda, *Nature*, 2003, **425**, 145.
4 N. Hosono, T. Kajitani, T. Fukushima, K. Ito, S. Sasaki, M. Takata and T. Aida, *Science*, 2010, **330**, 808–811.
5 H. Finkelmann, E. Nishikawa, G. G. Pereira and M. Warner, *Phys. Rev. Lett.*, 2001, **87**, 015501.
6 K. Iwaso, Y. Takashima and A. Harada, *Nat. Chem.*, 2016, **8**, 625–632.
7 Q. Li, G. Fuks, E. Moulin, M. Maaloum, M. Rawiso, I. Kulic, J. T. Foy and N. Giuseppone, *Nat. Nanotechnol.*, 2015, **10**, 161–165.
8 Z. Shi, P. Peng, D. Strohecker and Y. Liao, *J. Am. Chem. Soc.*, 2011, **133**, 14699–14703.
9 O. S. Bushuyev, A. Tomberg, T. Friščić and C. J. Barrett, *J. Am. Chem. Soc.*, 2013, **135**, 12556–12559.
10 N. K. Nath, L. Pejov, S. M. Nichols, C. Hu, N. Saleh, B. Kahr and P. Naumov, *J. Am. Chem. Soc.*, 2014, **136**, 2757–2766.
11 C. L. van Oosten, C. W. M. Bastiaansen and D. J. Broer, *Nat. Mater.*, 2009, **8**, 677–682.
12 J. A. Lv, Y. Liu, J. Wei, E. Chen, L. Qin and Y. Yu, *Nature*, 2016, **537**, 179–184.
13 S. Palagi, A. G. Mark, S. Y. Reigh, K. Melde, T. Qiu, H. Zeng, C. Parmeggiani, D. Martella, A. Sanchez-Castillo, N. Kapernaum, F. Giesselmann, D. S. Wiersma, E. Lauga and P. Fischer, *Nat. Mater.*, 2016, **15**, 647–653.
14 E. Kizilkan, J. Strueben, A. Staubitz and S. N. Gorb, *Science Robotics*, 2017, **2**, eaak9454.
15 X. Lu, S. Guo, X. Tong, H. Xia and Y. Zhao, *Adv. Mater.*, 2017, **29**, 1606467.
16 O. M. Wani, H. Zeng and A. Priimägi, *Nat. Commun.*, 2017, **8**, 15546.
17 S. Lamsaard, S. J. Aßhoff, B. Matt, T. Kudernac, J. J. L. M. Cornelissen, S. P. Fletcher and N. Katsonis, *Nat. Chem.*, 2014, **6**, 229–235.
18 M. Yamada, M. Kondo, J. Mamiya, Y. Yu, M. Kinoshita, C. J. Barrett and T. Ikeda, *Angew. Chem., Int. Ed.*, 2008, **47**, 4986–4988.
19 K. M. Lee, M. L. Smith, H. Koerner, N. Tabiryan, R. A. Vaia, T. J. Bunning and T. J. White, *Adv. Funct. Mater.*, 2011, **21**, 2913–2918.
20 L. D. Zhang and P. Naumov, *Angew. Chem., Int. Ed.*, 2015, **54**, 8642–8647.
21 M. E. McConney, A. Martinez, V. P. Tondiglia, K. M. Lee, D. Langley, I. I. Smalyukh and T. J. White, *Adv. Mater.*, 2013, **25**, 5880–5885.
22 L. Zhang, H. Liang, J. Jacob and P. Naumov, *Nat. Commun.*, 2015, **6**, 7429.

23 R. Tang, Z. Liu, D. Xu, J. Liu, L. Yu and H. Yu, *ACS Appl. Mater. Interfaces*, 2015, **7**, 8393–8397.
24 J. J. Wie, D. H. Wang, V. P. Tondiglia, N. V. Tabiryan, R. O. Vergara-Toloza, L. S. Tan and T. J. White, *Macromol. Rapid Commun.*, 2014, **35**, 2050–2056.
25 G. Ugur, J. Chang, S. Xiang, L. Lin and J. Lu, *Adv. Mater.*, 2012, **24**, 2685–2690.
26 H. M. D. Bandara and S. C. Burdette, *Chem. Soc. Rev.*, 2012, **41**, 1809–1825.
27 S. Wu, L. Niu, J. Shen, Q. Zhang and C. Bubeck, *Macromolecules*, 2009, **42**, 362–367.
28 S. Wu, Q. Zhang and C. Bubeck, *Macromolecules*, 2010, **43**, 6142–6151.
29 T. Ikeda and O. Tsutsumi, *Science*, 1995, **268**, 1873–1875.
30 H. Zhou, C. Xue, P. Weis, Y. Suzuki, S. Huang, K. Koynov, G. K. Auernhammer, R. Berger, H. J. Butt and S. Wu, *Nat. Chem.*, 2017, **9**, 145–151.
31 Z. Wang and Y. Liao, *Nanoscale*, 2016, **8**, 14070–14073.
32 Y. Zhao and J. He, *Soft Matter*, 2009, **5**, 2686–2693.
33 H. Zeng, B. Zhao, J. N. Israelachvili and M. Tirrell, *Macromolecules*, 2010, **43**, 538–542.
34 J. He, B. Yan, L. Tremblay and Y. Zhao, *Langmuir*, 2011, **27**, 436–444.
35 R. Yin, W. Xu, M. Kondo, C. C. Yen, J. I. Mamiya, T. Ikeda and Y. Yu, *J. Mater. Chem.*, 2009, **19**, 3141–3143.
36 F. Cheng, Y. Zhang, R. Yin and Y. Yu, *J. Mater. Chem.*, 2010, **20**, 4888–4896.
37 Y. Liu, W. Wu, J. Wei and Y. Yu, *ACS Appl. Mater. Interfaces*, 2017, **9**, 782–789.
38 A. A. Beharry, O. Sadovski and G. A. Woolley, *J. Am. Chem. Soc.*, 2011, **133**, 19684–19687.
39 D. Bléger, J. Schwarz, A. M. Brouwer and S. Hecht, *J. Am. Chem. Soc.*, 2012, **134**, 20597–20600.
40 S. Samanta, A. Babalhavaeji, M. X. Dong and G. A. Woolley, *Angew. Chem., Int. Ed.*, 2013, **52**, 14127–14130.
41 C. Knie, M. Utecht, F. L. Zhao, H. Kulla, S. Kovalenko, A. M. Brouwer, P. Saalfrank, S. Hecht and D. Bléger, *Chem.–Eur. J.*, 2014, **20**, 16492–16501.
42 P. Weis, D. Wang and S. Wu, *Macromolecules*, 2016, **49**, 6368–6373.
43 D. Wang, M. Wagner, A. K. Saydjari, J. Mueller, S. Winzen, H. J. Butt and S. Wu, *Chem.–Eur. J.*, 2017, **23**, 2628–2634.
44 D. Wang, M. Wagner, H. J. Butt and S. Wu, *Soft Matter*, 2015, **11**, 7656–7662.
45 D. Wang and S. Wu, *Langmuir*, 2016, **32**, 632–636.
46 P. Weis and S. Wu, *Macromol. Rapid Commun.*, 2018, **39**, 1700220.
47 K. Kumar, C. Knie, D. Bléger, M. A. Peletier, H. Friedrich, S. Hecht, D. J. Broer, M. G. Debije and A. P. Schenning, *Nat. Commun.*, 2016, **7**, 11975.
48 X. Chen, X. Han and Q. D. Shen, *Adv. Electron. Mater.*, 2017, **3**, 201600460.
49 W. Tong, Y. Zhang, Q. Zhang, X. Luan, F. Lv, L. Liu and Q. An, *Adv. Funct. Mater.*, 2015, **25**, 7029–7037.
50 H. Kawai, *Jpn. J. Appl. Phys.*, 1969, **8**, 975–976.
51 H. Zeng, O. M. Wani, P. Wasylczyk, R. Kaczmarek and A. Priimägi, *Adv. Mater.*, 2017, **29**, 1701814.